Effect of electric field on structure and dynamics of bilayers formed from anionic phospholipids

Madrid, Elena; Horswell, Sarah L.

DOI:
10.1016/j.electacta.2014.01.035

Document Version
Publisher's PDF, also known as Version of record

Citation for published version (Harvard):
Madrid, E & Horswell, SL 2014, 'Effect of electric field on structure and dynamics of bilayers formed from anionic phospholipids', *Electrochimica Acta*, vol. 146, pp. 850-860. https://doi.org/10.1016/j.electacta.2014.01.035

Electrochimica Acta 146 (2014) 850–860

Contents lists available at ScienceDirect

Electrochimica Acta

journal homepage: www.elsevier.com/locate/electacta

Effect of Electric Field on Structure and Dynamics of Bilayers Formed From Anionic Phospholipids☆

Elena Madrid[2], Sarah L. Horswell*,[1]

School of Chemistry, University of Birmingham, Edgbaston, Birmingham B15 2TT, UK

ARTICLE INFO

Article history:
Received 3 October 2013
Received in revised form
25 November 2013
Accepted 6 January 2014
Available online 21 January 2014

Keywords:
Adsorption, Phospholipid
Biomimetic membrane
Spectroelectrochemistry
Infrared spectroscopy

ABSTRACT

The effect of molecular structure on ensemble structure and dynamics of phospholipid bilayers has been investigated. Bilayers of dimyristoyl phosphatidylserine (DMPS) supported on Au(111) surfaces were prepared by Langmuir-Blodgett and Langmuir-Schaeffer deposition and studied with a combination of electrochemical measurements and *in situ* Polarisation Modulation Infrared Reflection Absorption Spectroscopy (PM-IRRAS). DMPS bilayers have relatively large capacitance when compared with those formed from similar molecules and this is attributed to a high solvent content within the bilayer, resulting from the need for solvation of the negatively charged lipid headgroups. Infrared spectra show that the ensemble of molecules is in a gel state, with extended and ordered hydrocarbon chains, similarly to bilayers of dimyristoyl phosphatidylethanolamine (DMPE) molecules, which are of similar shape. The infrared spectra also show that, in contrast to DMPE, the headgroups of DMPS are very strongly hydrated and have higher mobility. This higher mobility allows the re-orientation of the molecules under the influence of an applied electric field: re-orientation both of headgroups and hydrocarbon tail groups is observed. Thus the shape and charge of the molecules in an ensemble have a strong influence on both their structure and dynamics in the presence of an externally applied electric field.

1. Introduction

Phospholipids are a major component of biological cell membranes, self-assembling to form a fluid, selective barrier between the intracellular and extracellular fluids. Embedded within this lipid matrix are proteins and other lipids, which serve a range of functions, such as to control selective transport in and out of the cell and signalling between cells [1]. Consequently, there is a need and a strong interest to understand the properties of phospholipid bilayers and how these may be affected by their structure at the molecular level [2].

Studies of the electrical properties of lipid membranes have traditionally been carried out using patch clamp capacitance measurements [3,4], conductivity, capacitance and ac impedance of bilayer phospholipid membranes [5–10]. The action of ion channel-forming peptides can also be studied in this way [5,9,10]. A different approach to the study of phospholipid films has involved supporting a lipid monolayer on a mercury drop electrode, which is pushed through a phospholipid monolayer on an aqueous subphase [11–20]. The hydrophobic nature of Hg and the direction of deposition tend to lead to a monolayer with the hydrocarbon chains facing the metal surface and the hydrophilic headgroups facing the aqueous phase, although it is possible to invert the monolayer by application of a strong electric field [11]. These studies have involved investigating these potential-induced phase transitions of lipid layers with differential capacitance, ac impedance spectroscopy, coulometry and ion reduction [11–16], as well as determining surface charge density and surface dipoles of neutral and charged monolayers [17–20]. Interactions of the monolayers with ion channel-forming peptides [16,21–23] and the redox mechanism of ubiquinone within monolayers, mimicking the natural environment of ubiquinone [24,25], have been studied. Lipid films have also been made on solid supports, allowing the application of surface-sensitive probes such as vibrational spectroscopy [26–35], atomic force microscopy [36–40], scanning tunnelling microscopy [41,42] and reflectivity [38,43–45] to study the structure of model membranes at the molecular level. Solid-supported lipid membranes can be formed *via* the fusion of small unilamellar vesicles [26–28,36,37,40,41,43,44,46] or *via* Langmuir-Blodgett methods [29,31,47,48]. The use of vesicles is technically simpler and is sometimes better suited to the incorporation of peptides within films. On the other hand, Langmuir-Blodgett techniques afford more control

* Corresponding author. Tel.: +44 0 121 414 7474.
E-mail address: s.l.horswell@bham.ac.uk (S.L. Horswell).
[1] ISE member
[2] Department of Chemistry, University of Bath, Claverton Down, Bath BA2 7ZA, UK

0013-4686/$ – see front matter © 2014 The Authors. Published by Elsevier Ltd. All rights reserved.
http://dx.doi.org/10.1016/j.electacta.2014.01.035

over the structure of the biomimetic membranes, since molecules can be deposited at a fixed surface pressure (hence a better defined area per molecule), which results in fewer defects, and control over the composition of each layer is assured, at least initially.

Recent studies have shown that it is possible to study the structure of phospholipid films under potential control by supporting them on solid electrodes. This approach enables the investigation of electrical barrier properties, as in the case of Hg-supported monolayers, and allows the simultaneous acquisition of structural information under potential control [2]. Electrochemical measurements provide quantitative information on adsorption behaviour and the range of electric field strength within which the films are stable [2,28,29,43]. *In situ* infrared spectroscopic measurements have provided details of molecular orientation and packing as a function of applied field [26–29], scanning probe microscopies have provided information on molecular adsorption and arrangement [39,41,42] and *in situ* neutron reflectivity measurements have been used to determine quantitatively the degree of solvent ingress into the membranes as the applied field is varied [43,44]. Taken together, this information can be used to build up a detailed picture of how the structure of a lipid film affects its properties and the mechanism by which the film desorbs from the surface. This type of study also has potential to shed light on the mechanism of electroporation, a process that has applications in treatment of disease, for example, drug delivery and gene therapy [49,50].

Most work to date has been performed on the phosphatidylcholines and on mixtures of phosphatidylcholines with other species, such as cholesterol, glycolipids and ion channel-forming peptides. In natural cells, there is a wide range of lipid types, which may be present in different amounts in different types of membrane [1]. For example, there is a higher proportion of anionic phospholipids in bacterial cell membranes than in mammalian cell membranes [1]. The purposes of the different types of lipids are not yet well understood, although some are implicated in binding of proteins to cell membranes [1,51] and anionic lipids bind cations in the cytosol, which may be important in membrane fusion processes [52,53]. Consequently, it is essential to understand model systems composed of different lipids and their mixtures. Not only would this increase the depth of our understanding of biological systems, it would also facilitate the building of more complex architectures and the rational design of biomimetic systems. We have recently used a combination of electrochemical measurements and *in situ* Polarisation Modulation Infrared Reflection Absorption Spectroscopy (PM-IRRAS) to show that the shape of the phospholipid molecule has a profound impact on the physicochemical properties of the membrane formed [54]. Films formed from dimyristoylphosphatidylethanolamine (DMPE), depicted in Fig. 1, show enhanced electrical barrier properties because the cylindrical shape of the molecule enables molecules to pack closely together in a highly ordered structure with limited mobility and low solvent content. Films formed from DMPE were slightly thicker than films formed from the related dimyristoylphosphatidylcholine (DMPC), which is wedge-shaped, owing to the smaller tilt of the hydrocarbon chains from the surface normal. The DMPE molecules were also able to knit closely together through intermolecular hydrogen bonding between headgroups. In the present work, we show that the charge of the lipid has an important rôle to play in the structure and properties of the resulting film. Dimyristoylphosphatidylserine (DMPS), also shown in Fig. 1, has a similar size and shape to DMPE but its headgroup bears a negative charge, unlike DMPE, which is zwitterionic. The presence of the charge on the molecules leads to a difference in solvation, which has an impact on the electrochemical properties of the film and on the degree to which an applied electric field can cause changes in molecular organisation.

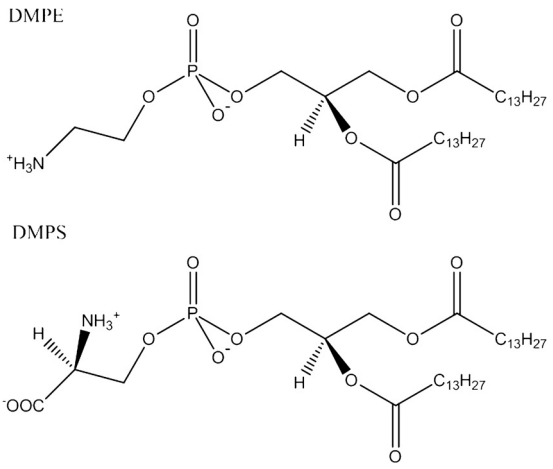

Fig. 1. Molecular structures of di-myristoyl phosphatidyl ethanolamine (DMPE) and di-myristoyl phosphatidyl serine (DMPS).

2. Experimental

2.1. Materials

Solutions of dimyristoylphosphatidyl-L-serine (DMPS) were prepared from DMPS (Avanti Polar Lipids, sodium salt, used as received) and a 1:9 mixture of methanol and chloroform (both HPLC grade, Sigma Aldrich).

All water used was purified with a tandem Elix-MilliQ Gradient A10 system (resistivity 18 MΩ cm, TOC < 5 ppb). Electrolyte solutions were made to a 0.1 M concentration with sodium fluoride (Suprapur grade, VWR) and ultrapure water or, for some of the PM-IRRAS measurements, deuterium oxide (99.99% D, Sigma Aldrich).

All glassware was cleaned by heating in a 1:1 mixture of concentrated sulphuric and nitric acids for at least 1 h, followed by rinsing thoroughly with ultrapure water and soaking in ultrapure water. Teflon, Kel-F parts and viton o-rings were cleaned with a 1:1 mixture of hydrogen peroxide and ammonia for several hours, rinsed with copious amounts of ultrapure water and soaked in ultrapure water. Spectroelectrochemical cell parts were dried in an oven prior to use.

2.2. Langmuir trough measurements

A teflon trough equipped with Delrin barrier and a dipper (Nima) was employed to record isotherms of floating monolayers and to deposit bilayers on Au surfaces. The trough and barrier were cleaned with chloroform, filled with ultrapure water and an isotherm was recorded to check for any contamination. 30 mL of a 1 mg mL^{-1} solution of DMPS was deposited onto the clean water/air interface and allowed to equilibrate. Isotherms were recorded with a barrier speed of 25 cm^2 s^{-1}. Fig. 2 shows the pressure-area isotherm recorded for a DMPS monolayer at the air|water interface. The isotherm shows a liquid condensed (L_c) phase and a solid (S) phase; the solid phase portion of the isotherm can be extrapolated back to give a limiting molecular area of ~40 Å^2; for comparison, the molecular area of DMPS in multilayers in the absence of salt has been reported to be 41 Å^2 [55] and the limiting molecular area of DMPS on a buffer sub-phase has also been reported at 41 Å^2 [56].

When a deposition was required, the cleaned Au substrate was placed below the surface of the water prior to deposition of the lipid monolayer on the water surface. The substrate was raised through the interface at a rate of 2 mm min^{-1} and at a target pressure of 48 mN m^{-1} (which corresponds approximately to the limiting molecular area of 40 Å^2). The monolayer thus formed was

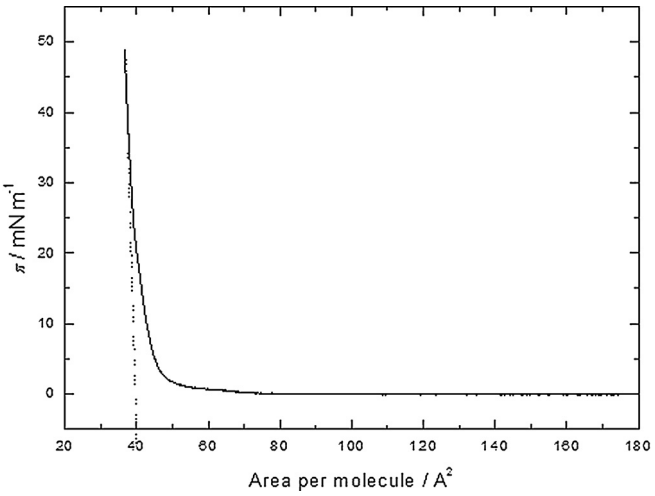

Fig. 2. Pressure-area isotherm for DMPS at the air/water interface. $T = 18^{\circ}C$.

dried in argon for 30 min and a Langmuir-Schaeffer deposition was performed, also at 48 mN m^{-1}. This type of deposition is a Y-type deposition.

2.3. Electrochemical measurements

A standard all-glass three electrode cell was employed for electrochemical measurements. The working electrode was a Au(111) single crystal oriented to better than 0.5° (Mateck, Germany) and was prepared as described previously [57] by annealing in a bunsen flame and rinsing with ultrapure water, before being transferred to the electrochemical cell with a drop of ultrapure water. After the electrochemical response of the clean surface had been checked, this electrode was transferred to the Langmuir trough for film deposition. The film was placed into the electrochemical cell immediately after deposition. The counter electrode was a Au coil (99.999%, Alfa Aesar) and was prepared by annealing in a bunsen flame and quenching with ultrapure water. The reference electrode was a saturated calomel electrode (SCE, Hach Lange). (However, because a Ag|AgCl|3 M KCl electrode was used for *in situ* PM-IRRAS measurements, all potentials quoted in this work will be reported with respect to the Ag|AgCl reference electrode.) 0.1 M NaF was used as electrolyte and was purged of oxygen for at least 45 min prior to measurements. An argon blanket was maintained above the solution throughout all measurements.

Differential capacity measurements were carried out with a Heka PGSTAT590 (Heka, Germany), connected to a 7265 DSP lock-in amplifier (Ametek) and to a PC *via* a data acquisition board (National Instruments). The software used to acquire the data was kindly provided by Dr. Alexei Pinheiro (Universidade Tecnologica Federal do Parana, Londrina, Brazil). A 20 Hz, 5 mV (r.m.s) ac signal was superimposed on a 5 mV s^{-1} potential ramp and the in-phase and quadrature components of the ac response were used to calculate the capacitance. Chronocoulometry measurements consisted of a series of potential steps, controlled by the computer software. The method used was similar to that described by Lipkowski *et al.* [29]. The potential was held at a base potential of–0.1 V for 60 s. (This potential was chosen by reference to the differential capacity curve.) Next, the potential was stepped to the potential of interest and held for 3 min, the time required for equilibrium to be reached. A brief step (0.15 s) was made to a potential sufficiently negative to desorb the molecules (again, determined from the differential capacity data) and returned to the base potential. Current transients recorded during the desorption step were integrated to provide relative charge densities. These were then converted to absolute charge densities using the potential of zero charge (pzc) of the electrode determined in a separate differential capacitance experiment in 5 mM NaF.

2.4. Infrared measurements

A Bruker Vertex80 v spectrometer was employed for infrared measurements. Data were collected with a liquid N_2-cooled MCT-A detector and at a resolution of 2 cm^{-1}. The spectrometer was equipped with an external, modified PMA50 module comprising a photoelastic modulator (PEM-100, Hinds Instruments, US) with a 50 kHz ZnSe optical head and a synchronous sampling demodulator (GWC Technologies, US) for PM-IRRAS measurements. PM-IRRAS measurements were carried out using a custom-built spectroelectrochemical cell with a BaF_2 equilateral prism as the window. A gold coil (99.999%, Alfa Aesar), concentric to the working electrode, was used as a counter electrode and the reference electrode was a Ag|AgCl|3 M KCl reference electrode (BASi, U.S.). A Au(111) crystal (99.999% purity, orientation <0.5°, Mateck, Germany) was used as the working electrode and was prepared as described above for the electrochemical measurements. The 0.1 M NaF electrolyte was prepared in either ultrapure water (for the lower wavenumber region when phosphate vibrations were investigated) or in deuterium oxide (when C–H and C=O stretching vibrations were investigated). The PEM was set for half-wave retardation at 2900 cm^{-1} for the C–H stretching region, at 1600 cm^{-1} for the C=O stretching region and at 1100 cm^{-1} for the phosphate stretching region. The optimum angles of incidence calculated by Zamlynny [58] for enhanced throughput were used. For the C–H stretching region, the angle of incidence was 51°, for the C=O stretching region, the angle of incidence was 60° and for the phosphate stretching region, the angle of incidence was 57°. The thickness of electrolyte between the window and the Au electrode was determined from reflectivity measurements as described by Zamlynny and Lipkowski [59] using software kindly provided by Prof. V. Zamlynny (Acadia University, Canada) [60]. The thicknesses used were ~2 μm for the C–H stretching region, ~2–3 μm for the C=O stretching region and ~1–2 μm for the phosphate stretching region.

The demodulation technique developed by Corn *et al.* [61,62] was employed and, to correct the intensity difference and average signals for the response of the PEM, a modification of the method described by Buffeteau *et al.* [63] was used. Once corrected in this way, the spectrum plots ΔS, which is related to the absorbance of the molecules by Eq. (1):

$$\Delta S = \frac{2\left(I_s - I_p\right)}{I_s + I_p} \approx 2.3\Gamma\varepsilon = 2.3A \quad (1)$$

where I_s and I_p are the intensities of the s- and p-polarised light, A is the absorbance, Γ is the surface concentration of the adsorbed species and ε is the molar absorption coefficient [64]. The method of background subtraction to correct for the PEM response has been described in detail by Lipkowski *et al.*, along with a spline interpolation technique to background-correct the resulting spectra [64]; the methods reported were used for the processing of the spectra reported in the present work.

Eq. (1) shows that the optical constants of the molecules under investigation need to be acquired if the PM-IRRA spectra are to be interpreted quantitatively. These can be obtained from separate transmission IR experiments. Transmission experiments were carried out in a liquid cell utilizing BaF_2 windows separated with a 10 μm teflon spacer. Spectra were measured in solutions of 0.1 M NaF in ultrapure water and 0.1 M NaF in deuterium oxide. The transmission spectra were used to calculate isotropic optical constants of DMPS in each solvent, employing software kindly provided by Zamlynny [60]. The optical constants were then used to simulate

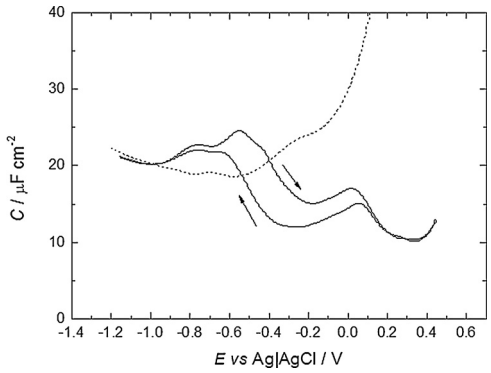

Fig. 3. Differential capacity curves for a Au(111) surface in 0.1 M NaF. Dotted line: in absence of lipids. Solid line: in presence of DMPS bilayer film. Potential scan rate 5 mV s^{-1}, r.m.s. amplitude 5 mV, ac frequency 20 Hz. The arrows indicate the direction of the potential sweep.

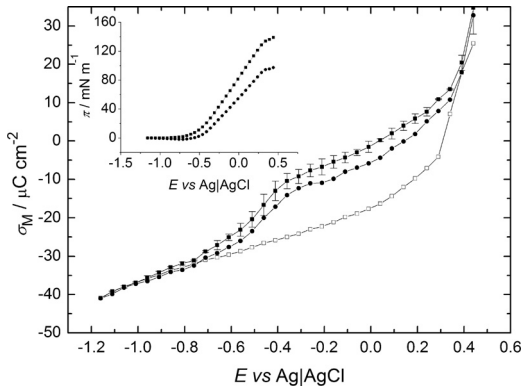

Fig. 4. Charge density curves for a Au(111) surface in 0.1 M NaF. Open points: in absence of film. Filled squares: in presence of DMPS bilayer film formed with LB-LS deposition. Filled circles: in presence of DMPS bilayer film formed from vesicle rupture. Error bars represent standard deviation between at least three independent measurements. Inset: Surface pressure-potential curve derived from integration of the charge density data.

PM-IRRA spectra of randomly oriented molecules for each of the cell configurations used in the spectroelectrochemical measurements. Typical errors in transition dipole tilt angle arising from background subtraction and deconvolution of spectra are around 4-5°.

3. Results and Discussion

3.1. Electrochemical results

The differential capacity recorded as a function of applied potential for the Au(111) surface coated with a bilayer of DMPS is shown in Fig. 3. At potentials negative of–0.95 V, the curve matches with that of the bare gold electrode, indicating that the DMPS molecules are desorbed in this potential range. Moving in the positive direction, a peak is observed, leading to a decrease in the capacity as compared with the base electrolyte for potentials positive of ~–0.6 V. A lower capacity for a bilayer-coated surface can be interpreted as resulting from an increase in the distance between the metal surface and the outer Helmholtz plane (OHP) and/or a decrease in the average permittivity of the interfacial region between the metal surface and the OHP. DMPS exhibits minimum capacity at the most positive potentials of 9–10 μF cm^{-2}. This capacity is higher than that reported for the similar molecules DMPC (7–8 μF cm^{-2}) [28] and DMPE (2–3 μF cm^{-2}) [54] and for that of bilayers of 9:1 DMPE:DMPS [44]. DMPS has a smaller headgroup than DMPC and might be expected to be oriented with its hydrocarbon chains tilted at an angle closer to the surface normal, which should result in a slightly thicker bilayer with lower capacities than observed for DMPC. DMPE has similar geometry to DMPS and exhibits lower capacity than DMPC [54]. Therefore, it seems that a decrease in thickness is unlikely to account for the relatively large capacity of a DMPS-coated electrode. It is more likely that the DMPS films contain relatively larger quantities of solvent, raising the average permittivity of the film. This could result from a large number of defects in the film or from a greater degree of hydration of the molecules. DMPS is an anionic molecule and would therefore be expected to be more hydrated than the zwitterionic molecules DMPC and DMPE.

Fig. 4 shows the chronocoulometric data for DMPS at a Au(111) electrode. Charge density-potential curves are compared for DMPS films formed by LB-LS deposition and vesicle fusion. The data are consistent with the differential capacity results, showing that an adsorbed film is formed at applied potentials between–0.4 V and +0.4 V. The corresponding range of charge density is approx.–14 μC cm^{-2} to +18 μC cm^{-2}, a little larger than that observed for electrically neutral molecules. The absolute charges measured for films formed by vesicle fusion are more negative than for those measured for films formed by the LB-LS technique. This can be understood by examining the area between the curve measured for a lipid-coated surface and the lipid-free surface. This area corresponds to the surface pressure of the bilayer, which is a measure of the lowering of the specific surface energy by the bilayer. The surface pressure, π, can be calculated with Eq. 2 [65]:

$$\pi = \gamma_0 - \gamma = \int_{E=-1.01V}^{E} \sigma_M dE - \int_{E=-1.01V}^{E} \sigma_{M_0} dE \quad (2)$$

The surface pressures for the LB-LS and vesicle bilayers are plotted in the inset to Fig. 3. The surface pressure for the film produced by vesicle fusion is lower than that for the film prepared by LB-LS deposition. This suggests that the surface density of lipids is lower for films prepared from vesicles, which might indicate a higher density of defects and/or incomplete rupturing of vesicles. For this reason, further analysis was carried out on bilayers prepared by the LB-LS technique.

A small negative shift in the potential of zero charge is observed when DMPS is adsorbed on the Au surface. The shift is a little larger than that observed for bilayers formed from zwitterionic phospholipids [29,54] but much smaller than that observed by Burgess *et al.* for monolayers of the anionic surfactant sodium dodecyl sulphate (SDS) on Au(111) (*ca* –0.125 V for hemimicellar aggregates and extrapolated to give–7.8 V for a condensed film with headgroups facing the surface) [66]. Burgess *et al.* discussed the likely shift for different arrangements of the anionic surfactant, including a bilayer with half of the molecules oriented with their heads towards the surface and half of the molecules with their tails towards the surface, which is similar to the arrangement of the DMPS layers in the present study, although with more interdigitation of hydrocarbon chains [66]. For this arrangement, the potential drop between the charged headgroups adjacent to the surface and the solvated counter-ions in the OHP was likely to be largest and the shift in the pzc for this arrangement of molecules was also expected to be substantial. The notably smaller shift observed for DMPS bilayers than for SDS layers suggests that the molecules do not adsorb as anions but rather as ion pairs (the sodium counter-ion may remain associated with the headgroups) or that a significant degree of shielding takes place (from solvent or ions). The presence of a shift would then indicate that there is an asymmetry in charge distribution across the bilayer. The small shift is not surprising: studies of DOPS monolayers supported at mercury surfaces exhibited similar surface charge densities as DOPE and DOPC monolayers [18], although

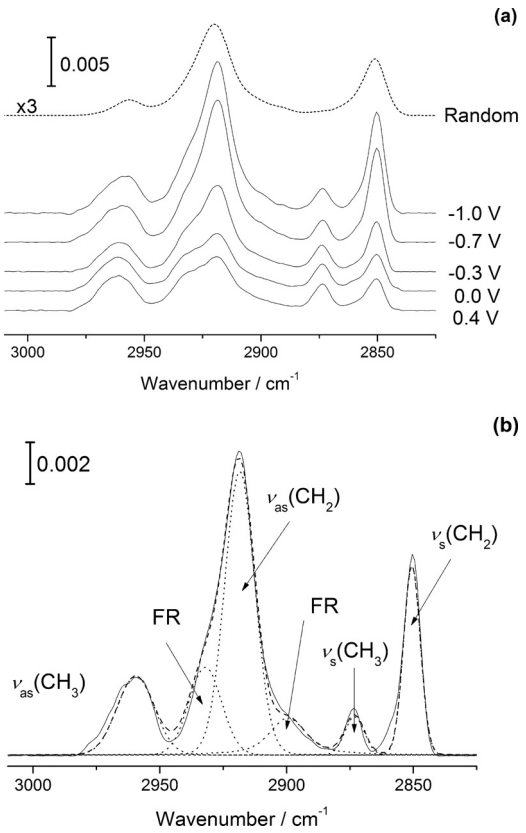

Fig. 5. (a) Selected PM-IRRA spectra in the C-H stretching region at the indicated applied potentials. Dotted line: simulated spectrum of randomly oriented molecules under the same experimental conditions (scaled for clarity). (b) Example of deconvolution of the spectrum acquired at–0.7 V. Dotted lines represent each peak, the dashed line is the cumulative fit and the solid line traces the data. The angle of incidence was 51.1° and the electrolyte thickness 2.1 μm.

it should be noted that DOPS layers would be expected to have lower charge density than DMPS layers, owing to the larger average size of the constituent molecules [53]. A further difference to note between the behavior of SDS and DMPS is the fact that the capacitance of DMPS layers is significantly higher than that of SDS in the positive potential region. Given that the thickness of the DMPS bilayer is expected to be similar to that of a DMPE bilayer (the molecular geometries are similar), it is most likely that the high capacitance is indicative of a higher degree of solvent content.

3.2. PM-IRRAS measurements

3.2.1. C–H stretching region

Fig. 5a shows selected spectra acquired in the C–H stretching region at various applied electrode potentials. Also shown (as a thicker line) is a spectrum calculated for a film of randomly adsorbed molecules. Pronounced changes in the spectra occur as the applied field is varied: most obvious is the change in intensity of the methylene symmetric and antisymmetric vibrations at ~2852 cm^{-1} and ~2919 cm^{-1}, respectively. The vibrations observed at ~2870 cm^{-1} and ~2965 cm^{-1} correspond, respectively, to symmetric and antisymmetric vibrational modes of methyl groups in the hydrocarbon chains [31,52,53,67–78]. Two more bands are observed in this region that correspond to Fermi resonances between C–H stretching bands and overtones of C–H bending modes [69,70,79]. For detailed analysis of the spectra, each spectrum must be deconvoluted into the six bands. An example of the deconvolution is provided in Fig. 5b. The position of the CH_2 stretching vibrations provides information on the average conformation of the hydrocarbon chains and the full width half-maximum (FWHM) provides information on the mobility and ordering of the molecules within the film. Fig. 6 shows the dependence of these quantities on the applied potential. Data obtained for DMPE are included for comparison. At negatively charged surfaces, the average band centres are 2850.6 cm^{-1} and 2918.4 cm^{-1}, indicative of hydrocarbon chains in the gel state [52,69–71,74,76]. As the charge density on the surface is reduced, the wavenumbers of the bands increase to 2850.9 cm^{-1} and 2919.4 cm^{-1}, indicating that the average number of *gauche* conformers increases slightly [52,53,69–71,74,76]. The band position and FWHM of the antisymmetric stretch are both higher at the more positive potentials than at the negative potentials, indicating that the film is more ordered with less mobility at the negatively charged surface. Although the changes are small (within the resolution employed), the trend is clear. This behaviour is similar to that of LB-LS films of the related molecule DMPC [29], although, as Fig. 6 shows, films of DMPE display a smaller change [54]. The band centres and FWHM of DMPS films are lower than those of DMPE films and DMPC films, indicating more ordering in DMPS films.

The integrated intensities of the bands are related to the tilt angles of the transition dipoles from the normal to the surface:

$$\int Adv \quad \alpha\, |\boldsymbol{\mu}.\boldsymbol{E}|^2 = |\mu|^2 \langle E \rangle^2 \cos^2\theta \tag{3}$$

where A is the absorbance, μ is the dipole moment, E is the electric field vector and θ is the angle between the direction of the transition dipole moment and the normal to the surface [64,80]. The area under the band is also related to the amount of material present. The tilt angle θ can be calculated by comparing the integrated band intensity of the supported bilayer with the band intensity in a simulated spectrum, calculated for a film of the same thickness of randomly oriented molecules [64,81,82]:

$$\cos^2\theta = \frac{1}{3}\frac{\int_E Adv}{\int_{random} Adv} \tag{4}$$

Fig. 7 shows a plot of the tilt angle of the transition dipole moments of the CH_2 symmetric and antisymmetric stretches as a function of the applied potential. The tilt angles obtained for DMPE bilayers (taken from ref. 54) are included for comparison. The tilt angles of both DMPS symmetric and antisymmetric stretching mode transition dipole moments decrease dramatically as the applied potential is made more negative. The tilt angle of the backbone of the hydrocarbon chain can be calculated from these values using equation 5:

$$\cos^2\theta_s + \cos^2\theta_{as} + \cos^2\theta_{chain} = 1 \tag{5}$$

where θ_{as} is the tilt angle of the direction of the transition dipole moment corresponding to the antisymmetric stretching vibration, θ_s is the tilt angle of the direction of the transition dipole moment corresponding to the symmetric stretching vibration and θ_{chain} is the tilt angle of the hydrocarbon chain [83]. The dependence of this tilt angle on applied potential is also plotted in Fig. 7. The tilt angle of the chain increases from 17° to 30° as the potential is made more negative. Unlike DMPC, the DMPS molecules are oriented with their chains closer to the surface normal at positive potentials (low charge densities), whereas DMPC molecules are more tilted [29]. For DMPC, the relatively high tilt angle has been explained in terms of the orientation of the headgroups on the surface: the fact that the headgroup is larger in area than the cross-sectional area of the hydrocarbon chains means that the chains must tilt to reduce inter-chain distance and hence maximise dispersion interactions [28,29,43]. The headgroup of DMPS is smaller than that of DMPC, which means that the chains do not need to tilt as much to maximise dispersion interactions. The orientation of DMPS

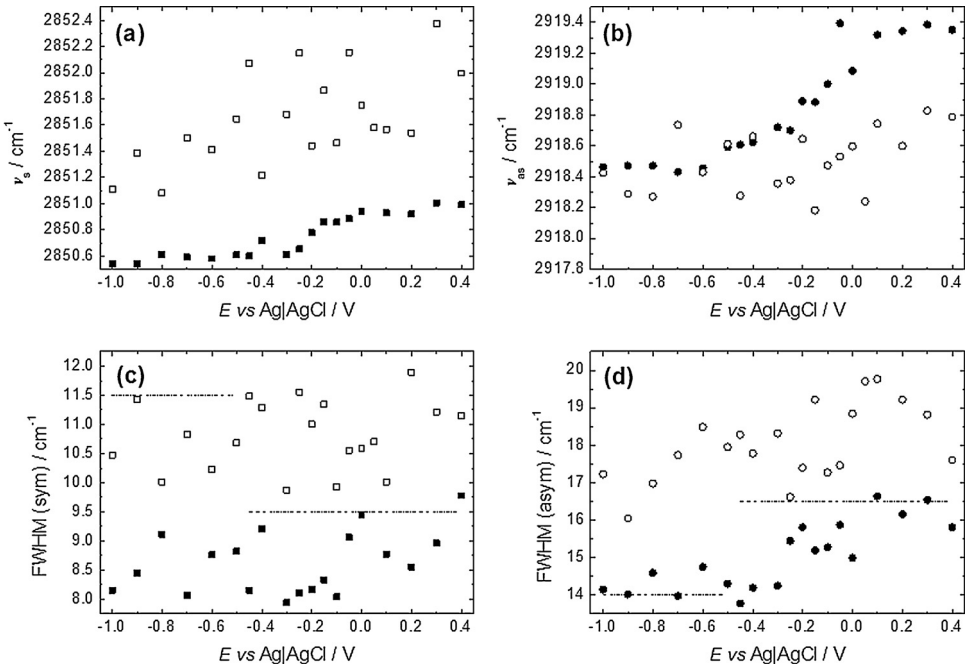

Fig. 6. Plots of CH_2 stretching mode peak positions and full-width half maxima (FWHM) as a function of applied potential. (a) C-H methylene symmetric stretch, (b) C-H methylene antisymmetric stretch, (c) FWHM symmetric stretch, (d) FWHM antisymmetric stretch. In each case, the filled shapes represent data acquired for DMPS bilayers and the open shapes represent data acquired for DMPE bilayers [average values were reported in 54]. For comparison, the dashed lines represent average values of FWHM obtained for DMPC bilayers prepared with the same method, taken from Zawisza *et al.* [29]. The average values of the band centres obtained for DMPC were reported as 2854 cm^{-1} and 2923 cm^{-1} at potentials negative of -0.5 V and 2852.5 cm^{-1} and 2922 cm^{-1} at potentials positive of -0.45 V [29].

hydrocarbon chains in the potential range where molecules are expected to be directly adsorbed is similar to that observed for DMPE, which has a headgroup of similar size [54]. Therefore, it seems likely that the similarities and differences in orientation of the tailgroups of the three molecules, when directly adsorbed on Au, at small charge densities, can be explained by geometric arguments. As the applied potential is made more negative, a smooth increase in chain tilt angle is observed, rising to a value of 30° at potentials negative of *ca* –0.4 V, corresponding to charge densities of *ca* –10 μC cm^{-2}. DMPC displayed the opposite trend, with a smooth decrease in chain tilt angle as the surface was made negatively charged: in that case, the headgroups were believed to adopt a zig-zag arrangement on a water cushion, allowing chains to adopt a more upright orientation [29]. In contrast, DMPE, which is more similar in shape to DMPS, displayed only a very small, monotonic rise across the potential range, from which we inferred that the tight packing of molecules was retained in both phases (at small and at large negative charge densities) as a result of strong intermolecular interactions [54]. The greater fluidity of the DMPC film and its lack of direct hydrogen bonding interactions enabled re-organisation of the headgroups. The difference in behaviour between DMPE and DMPS must result from the anionic nature of the DMPS headgroup because the molecular shape is similar and the headgroups of both molecules can take part in direct hydrogen bonding. It is likely that the anionic headgroups need to be screened by water when exposed to negative charge densities, which could result in quite different structures for the DMPC, DMPE and DMPS films in the negative potential region. Spectra corresponding to the ester and headgroup vibrations were next examined to gain insight into headgroup hydration and orientation.

3.2.2. *C=O stretching region*

Fig. 8 presents spectra corresponding to the ester C=O stretch, acquired at selected applied potentials. In each spectrum, a broad

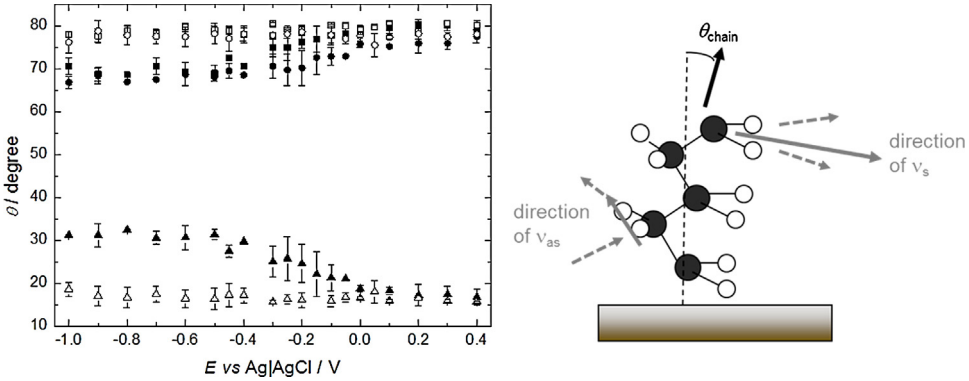

Fig. 7. Plot of tilt angles as a function of applied potential. The squares represent the tilt angles of the transition dipole of the CH_2 symmetric vibration, the circles represent the tilt angles of the transition dipole of the CH_2 antisymmetric vibration and the triangles represent the tilt angles of the direction along the hydrocarbon chain, with respect to the surface normal. The cartoon shows the relationship between the three directions. The filled shapes represent tilt angles measured for DMPS bilayers and the open shapes represent tilt angles measured for DMPE bilayers (the latter data taken from reference 54).

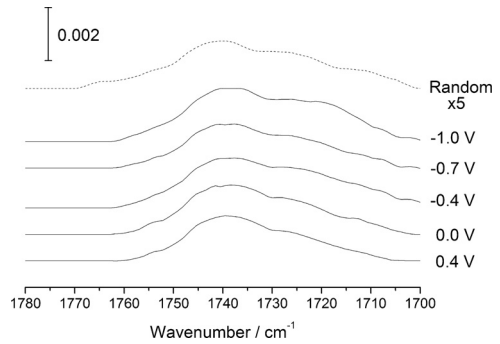

Fig. 8. Selected PM-IRRA spectra in the ester C = O stretching region at the indicated applied potentials. Dotted line: simulated spectrum of randomly oriented molecules under the same experimental conditions (scaled for clarity). The angle of incidence was 61.5° and the electrolyte thickness 2 μm.

band is observed, comprising at least two, possibly three components. The bands increase in intensity as the potential is varied in the negative direction, with the lower wavenumber components increasing most. Phospholipid aqueous dispersions have previously been shown to exhibit two or three broad bands in this region of the IR spectrum, although the origin of the different bands has been the subject of discussion [74]. Originally the existence of two bands was believed to arise from the conformational non-equivalence of the *sn*-1 and *sn*-2 ester groups [52,78] but experiments with molecules selectively labelled with $^{13}C=O$ esters showed that the difference in wavenumber associated with conformational non-equivalence is relatively small (~4 cm^{-1}). In these studies, the origin of two bands (at *ca* 1741 and 1721–1728 cm^{-1} for $^{12}C=O$) was shown to be related to hydration, with ester groups in a dehydrated environment vibrating at the higher wavenumber and those in a hydrated environment vibrating at the lower wavenumber (because hydrogen bonding to water lowers vibrational frequency) [77,84,85]. The peak centre or the relative intensities of the higher and lower wavenumber components is now used as an indication of the degree of hydration of the ester region of the phospholipid molecule [74,76,77]. Some studies have reported three bands in this region [53,76], with the lowest wavenumber assigned to a different environment, interaction with two water molecules or with amine groups of neighbouring molecules. Hence the bands observed in our spectra (at ~1740 cm^{-1}, ~1723 cm^{-1} and ~1712 cm^{-1}) can be assigned to the presence of carbonyl centres in three environments: two with a large degree of hydration and one relatively dehydrated. Fig. 9 presents the relative contribution of the "dehydrated"

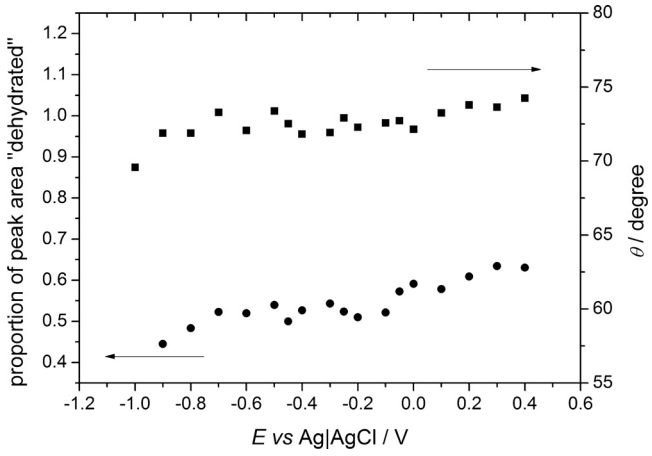

Fig. 9. Plot of average C = O transition dipole tilt angles (squares) and proportional area of the higher wavenumber component of the band (circles) as a function of applied potential.

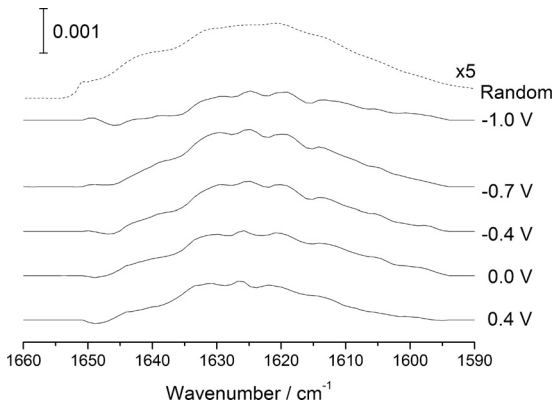

Fig. 10. Selected PM-IRRA spectra in the carboxylate C = O stretching region at the indicated applied potentials. Dotted line: simulated spectrum of randomly oriented molecules under the same experimental conditions (scaled for clarity). The angle of incidence was 61.5° and the electrolyte thickness 2 μm.

component of the C = O stretch as a function of applied potential. At negative potentials, this relative contribution decreases; *i.e.*, the lower wavenumber components increase in intensity relative to the higher wavenumber component, indicating that the hydration of the ester regions is greater at negative charge densities. This is consistent with the model proposed by Lipkowski *et al.* [28,29,43] of water ingress during the electrochemical phase transition. It is interesting to note that the extent of hydration of the ester groups is higher than that of DMPE, over the whole potential range (the "dehydrated" proportion for DMPS is 0.4–0.6, compared with ~0.7 for DMPE [54]). This reflects the fact that the anionic DMPS is easier to hydrate than DMPE, which has a strong intermolecular hydrogen bond network, and is consistent with the previous observation that hydrogen bonded ester groups are predominant for PS bilayers [76]. The observed increase in water content of our film could explain why the hydrocarbon chains tilt so strongly at highly negative charge densities: if the headgroups and interfacial regions were to occupy more area as a result of hydration, the hydrocarbon chains would need to tilt to increase their intermolecular dispersion interactions. The overall intensity of the ester bands changes as the potential is varied, indicating a change in the average orientation of the ester groups. These trends are presented in Fig. 9, which also shows the estimated average tilt angle of the ester C = O transition dipoles. This tilt angle should be regarded as an estimate because the band intensity can vary if the extent of hydrogen bonding varies. Nevertheless, it can be seen that the general trend is consistent with that of the tilt angle of the hydrocarbon chains: the transition dipole moment of the C = O band is expected to be perpendicular to the direction of the hydrocarbon chains; hence, if the C–H bands increase in intensity, so should the C = O band. The difference between the behaviour of the carbonyl and hydrocarbon groups is that the variation in the tilt angle of the carbonyl groups is more gradual across the potential range, whereas the tilt angle of the hydrocarbon chains changes in a shallow step.

The DMPS molecule also has a carboxylate moiety in its headgroup, which has a stretching vibration at ~1640 cm^{-1} (and another expected in the lower wavenumber region, 1150–1300 cm^{-1}). Spectra in this region are presented in Fig. 10. Similarly to the ester stretching vibration, the carboxylate vibration is sensitive to the degree of hydrogen bonding [52,86]. The band contour in Fig. 10 can be fitted to two mixed Gaussian-Lorenztian peaks, one at *ca* 1640 cm^{-1} and one at *ca* 1622 cm^{-1}, the former corresponding to relatively dehydrated carboxylate groups and the latter to carboxylate groups participating in a significant amount of hydrogen bonding [52,86]. The percentage contribution of the

former component is approximately 35%, indicating that the carboxylate groups are strongly hydrated.

3.2.3. Phosphate region

Vibrations of the phosphate group of DMPS are complex and a number of bands are present in the lower wavenumber region of the spectra. The bonds between free oxygen atoms and the phosphorus atom tend to give rise to an O-P-O antisymmetric stretching vibration between 1210-1260 cm^{-1} and a group of bands at approximately 1100 cm^{-1}, which is composed of O-P-O stretching vibrations and other stretching vibrations involving the oxygen atoms that are bound to the glycerol moiety and the serine group (P-O[C] vibrations). The wavenumbers of the O-P-O antisymmetric and symmetric modes give an indication of the degree of hydrogen bonding involving the free oxygen atoms, where lower wavenumbers are typical of strongly hydrated samples, and the FWHM gives information on the mobility of the headgroups, where a narrow bandwidth indicates relatively immobilised groups. In the spectral regions where the O-P-O antisymmetric stretching vibrations are expected, a number of bands were observed that have similar wavenumber to CH_2 wagging vibrations previously observed in the literature for low temperature DMPC and DMPE samples [87]. DMPC bilayers have not been reported to show this wagging mode progression under similar conditions to the present work, probably because the progression is most obvious for ordered samples where few *gauche* conformers are present and tend to fade as the temperature approaches the main chain melting phase transition [71,87,88]. This phase transition is 24°C for DMPC [67,89] and 39°C for sodium salts of DMPS [52]. The DMPS molecules in the present study should be in a gel state, below the phase transition, and will have ordered chains with few *gauche* conformers, which was indeed observed from the CH_2 stretching vibration bands. Hence, it is not unexpected to observe the CH_2 wagging mode progression for DMPS. We have also recently shown that DMPE bilayers show a wagging mode progression under these experimental conditions and concluded that the hydrocarbon chains in DMPE bilayers contained fewer *gauche* conformers than DMPC bilayers under similar conditions (as the chain melting phase transition for DMPE is 49–50°C, [68] resulting in a highly ordered solid phase at room temperature). In the case of DMPE, one of the bands had significantly higher intensity than the others but this is not the case for DMPS. Experiments with per-deuterated DMPE, for which the wagging vibrations are shifted to lower wavenumber, showed that the band at 1252 cm^{-1} had a contribution from the antisymmetric phosphate stretching vibration, which explained its relatively higher intensity. Unfortunately, the cost of per-deuterated DMPS precludes a similar experiment in this work. It is possible only to speculate that the similar intensities of the bands we observe suggest that the phosphate contribution to the spectra is small for DMPS, which indicates that the transition dipole of this vibration lies close to parallel to the Au(111) surface.

Fig. 11 presents spectra in the region where the symmetric O-P-O and P-O[C] stretching vibrations are expected. The dotted line shows a simulated spectrum of randomly oriented molecules, calculated from the optical constants acquired in water. A broad band is observed, that can be fitted to four components at ~1109 cm^{-1}, 1099 cm^{-1}, 1072 cm^{-1} and 1045 cm^{-1}. DMPC exhibits a similarly broad band that can be deconvoluted into its constituents [29] and spectra of DMPE bilayers contain much narrower bands, indicating less mobility of DMPE headgroups within supported bilayers [54]. The broad bands in the DMPS spectra in Fig. 11 show that the phosphate groups are more mobile than DMPE phosphate groups, which suggests that the intermolecular hydrogen bonding is weaker, perhaps as a result of greater hydration. The FWHM of the bands do not change as the applied potential is varied. By comparison with spectra acquired for DMPC, the 1099 cm^{-1} band

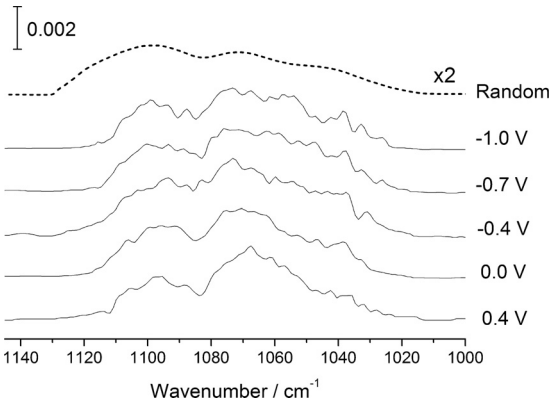

Fig. 11. Selected PM-IRRA spectra in the phosphate O-P-O symmetric stretching region at the indicated applied potentials. Dotted line: simulated spectrum of randomly oriented molecules under the same experimental conditions (scaled for clarity). The angle of incidence was 57° and the electrolyte thickness 1.3 μm.

is likely to correspond to the O-P-O symmetric stretching vibration [29,90] and the other three bands to P-O[C] vibrations. The splitting pattern is complex and difficult to interpret: the relative intensities could indicate particular orientation of the functional groups or different conformations of the [C]O-P-O[C] backbone. Studies that have been undertaken on the spectra of PS molecules, focusing on the effect of metal ion binding, showed a change in splitting on complexation of the metal ions to phosphate groups. Ammonium and sodium salts of DMPS were reported to produce a group of three bands at ~1100 cm^{-1}, with positions indicative of strong hydration, whereas PS molecules complexed with metal ions showed dehydration of the phosphate group (an increase in wavenumber as the metal-phosphate interaction replaced some of the water-phosphate interactions) but not of the carboxylate group. Complexation with a divalent metal ion resulted in spectra composed of four bands [52,53,78] and the patterns of lower wavenumber modes (inaccessible in our experiments) suggested bidentate complexes. The splitting pattern of the bands at ~1100 cm^{-1} was concluded also to be a marker for a bidentate complex of the PS phosphate group with a metal ion, which was rationalised by a change in the point group of the phosphate moiety, in line with similar observations for other polyatomic inorganic anions [78]. The only metal ion present in our study is Na^+, yet the spectra both for solution-based DMPS and DMPS bilayers are best fit with four bands. However, the appearance of our spectra is more akin to that of the spectra of hydrated DOPS [53] with a broader band at 1100–1110 cm^{-1} than to spectra of DOPS-Ca^{2+} complexes, whose bands are relatively starkly split [53]. In addition, the DMPS-NH_4^+ spectra reported in [52] consist of a broad peak containing three bands (1100, 1085, 1068 cm^{-1}) with another, smaller and slightly separated band, just below 1050 cm^{-1}, which are not dissimilar to our own spectra. The similarity with spectra observed previously for DMPC [29] suggests that the conformation of the [C]O-P-O[C] is similar for DMPS. However, the relative intensity of the lower wavenumber modes of DMPS compared with DMPC indicates that there may be a difference in orientation of the phosphate [C]O-P-O[C] backbones of the two molecules. Assuming that the 1099 cm^{-1} band corresponds to the O-P-O symmetric stretching vibration, its intensity can be used to estimate the tilt angle of this transition dipole moment (which bisects the O-P-O angle) from the surface normal. Fig. 12 plots this estimated tilt angle, along with that of the COO^- (antisymmetric) stretching mode (estimated from the areas of the bands in Fig. 10), as a function of applied potential. From these plots it is evident that the headgroup re-orients as the potential is made more negative but both transition dipoles regain their original tilt angle at the end of the

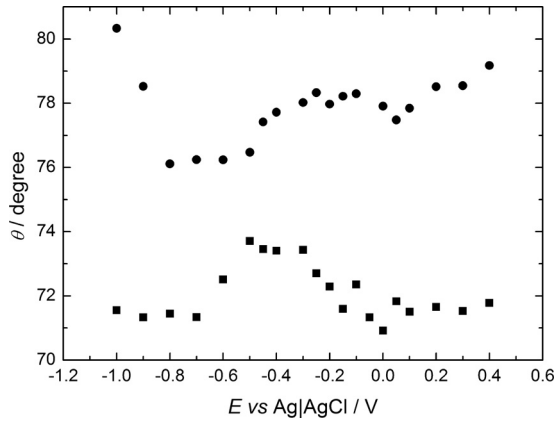

Fig. 12. Plots of angle made between the surface normal and the transition dipole moments of the phosphate symmetric stretching mode (squares) and carboxylate antisymmetric stretching mode (circles) as a function of applied potential/charge.

electrochemical phase transition. This re-orientation is concomitant with that of the hydrocarbon chains but the hydrocarbon chains remain tilted at negative potentials. The carboxylate group appears to re-orient again at the most negative potentials, where molecules are completely desorbed from the surface. These changes are interesting but difficult to interpret in the absence of tilt angles for the phosphate antisymmetric stretching vibration and carboxylate symmetric stretching vibration, which were hidden by CH_2 wagging vibrations. In addition, spectra cannot be acquired for NH_3^+ modes because of their overlap with water bending vibrations. (Note that replacement of H_2O with D_2O would simply result in exchange of H/D to give ND_3^+, whose bands would overlap with those of D_2O.) Acquisition of spectra of similar PS molecules (*e.g.* unsaturated PS) combined with simulations could shed light on this behaviour and will be the subject of future work. However, our spectra of the headgroup moieties have still demonstrated both that the headgroups re-orient as a result of the applied field and that the headgroups are both hydrated and mobile. This high degree of hydration provides an explanation for the relatively high capacitance observed in the electrochemical experiments.

4. Conclusions

Di-myristoyl phosphatidyl serine (DMPS) bilayers supported on Au electrodes have been studied with electrochemical and *in situ* PM-IRRAS measurements. The shape and charge of the molecule have a profound influence on the structure and properties of the bilayer. The headgroup footprint is of similar size to that of the hydrophobic tail groups, leading to ordered packing of molecules at small applied fields: PM-IRRA spectra indicate a high degree of ordering and a tail orientation similar to that observed for zwitterionic molecules of similar shape (DMPE). However, the electrochemical barrier properties of DMPS bilayers are significantly different from those of DMPE. This observation can be explained by a greater degree of hydration of DMPS, arising from its charge. PM-IRRA spectra show that the ester linkages and headgroups of DMPS are strongly solvated. The high solvent content would raise the average dielectric constant of the bilayer, resulting in a higher capacitance than for DMPE. In addition, our PM-IRRA spectra demonstrate a clear re-orientation of the headgroups as the applied potential is made more negative. The charge of the molecule evidently has an effect on both the structure and the dynamics of the ensemble, since DMPS undergoes re-orientation more readily than DMPE, which has similar size and shape. Our results thus show that the structure of a molecule has a significant impact on the properties of bilayer films that it forms, as a result of its effect on the structure of the bilayer films. These results have implications for the design of biomimetic films for use in the study of biologically active molecules or for sensing devices. Although pure DMPS films appear not to be suited to these applications, the understanding gained from this study of the behaviour of this lipid is vitally important because PS has been implicated in a range of biological functions in cells [1,52,53,76] and this work is an important step toward studies of biomimetic films containing a proportion of anionic lipids.

Acknowledgements

This work was supported by EPSRC (grant number EP/D05561X/1) and by the Royal Society (Small Equipment Grant). EM is grateful to the School of Chemistry, University of Birmingham, for a studentship. The authors are indebted to Prof. V. Zamlynny and Prof. J. Lipkowski for helpful discussions about the experimental set-up and for kindly allowing us to use the Fresnel software. The technical advice and support of Prof. T. Rayment, Mr A. Rothin, Mr S. Williams and Mr S. G. Arkless is gratefully acknowledged, as is the help of Dr A.L.N. Pinheiro with the data acquisition software.

References

[1] B. Alberts, A. Johnson, J. Lewis, M. Raff, K. Roberts, P. Walter, Molecular Biology of the Cell, 4th Ed., Taylor and Francis, 2002, Ch 10.
[2] J. Lipkowski, Building biomimetic membrane at a gold electrode surface, Phys. Chem. Chem. Phys 12 (2010) 13874–13887.
[3] L.J. Breckenridge, W. Almers, Currents through the fusion pore that forms during exocytosis of a secretory vesicle, Nature 328 (1987) 814–817.
[4] K. Debus, J. Hartmann, G. Kilic, M. Lindau, Influence of conductance changes on patch clamp capacitance measurements using a lock-in amplifier and limitations of the phase tracking technique, Biophys. J. 69 (1995) 2808–2822.
[5] E. Bamberg, R. Benz, Voltage-induced thickness changes of lipid bilayer membranes and effect of an electric-field on gramicidin A channel formation, Biochim. Biophys. Acta 426 (1976) 570–580.
[6] G. Krishna, J. Schulte, B.A. Cornell, R. Pace, L. Wieczorek, P.D. Osman, Tethered bilayer membranes containing ionic reservoirs: The interfacial capacitance, Langmuir 17 (2001) 4858–4866.
[7] R. Cohen, B.M. Schmitt, D. Atlas, Molecular identification and reconstitution of depolarization-induced exocytosis monitored by membrane capacitance, Biophys. J. 89 (2005) 4364–4373.
[8] E.L. Florin, H.E. Gaub, Painted supported lipid membranes, Biophys. J. 64 (1993) 375–383.
[9] A. Hirando-Iwata, A. Oshima, T. Nasu, T. Taira, Y. Kimura, M. Niwano, Stable lipid bilayers based on micro- and nano-fabrication, Supramol. Chem. 22 (2010) 406–412.
[10] A. Studer, X. Han, F.K. Winkler, L.X. Tiefenauer, Formation of individual protein channels in lipid bilayers suspended in nanopores, Coll. Surf. B 73 (2009) 325–331.
[11] A. Nelson, F.A.M. Leermakers, Substrate-induced structural changes in electrode-adsorbed lipid layers: Experimental evidence from the behaviour of phospholipid layers on the mercury–water interface, J. Electroanal. Chem. 278 (1990) 73–83.
[12] D. Bizzotto, A. Nelson, Continuing electrochemical studies of phospholipid monolayers of dioleoyl phosphatidylcholine at the mercury–electrolyte interface, Langmuir 14 (1998) 6269–6273.
[13] C. Whitehouse, R. O'Flanagan, B. Lindholm-Sethson, B. Movaghar, A. Nelson, Application of electrochemical impedance spectroscopy to the study of dioleoyl phosphatidylcholine monolayers on mercury, Langmuir 20 (2004) 136–144.
[14] A. Nelson, Electrochemistry of mercury supported phospholipid monolayers and bilayers, Curr. Opin. Coll. Interf. Sci. 15 (2010) 1455–1466.
[15] M. Rueda, I. Navarro, F. Prieto, A. Nelson, Impedance measurements with phospholipid-coated mercury electrodes, J. Electroanal. Chem. 454 (1998) 155–160.
[16] M. Rueda, F. Prieto, I. Navarro, R. Romero, Phospholipid and gramicidin-phospholipid-coated mercury electrodes as model systems of partially blocked electrodes, J. Electroanal. Chem. 649 (2010) 42–47.
[17] R. Guidelli, G. Aloisi, L. Becucci, A. Dolfi, M.R. Moncelli, F.T. Buoninsegni, Bioelectrochemistry at metal | water interfaces, J. Electroanal. Chem. 504 (2001) 1–28.
[18] L. Becucci, M.R. Moncelli, R. Herrero, R. Guidelli, Dipole potentials of monolayers of phosphatidylcholine, phosphatidylserine and phosphatidic acid on Mercury, Langmuir 16 (2000) 7694–7700.
[19] M.R. Moncelli, L. Becucci, F.T. Buoninsegni, R. Guidelli, Surface dipole potential at the interface between water and self-assembled monolayers of phosphatidylserine and phosphatidic acid, Biophys. J. 74 (1998) 2388–2397.
[20] F.T. Buoninsegni, L. Becucci, M.R. Moncelli, R. Guidelli, Total and free charge densities on mercury coated with self-assembled phosphatidylcholine and

octadecanthiol monolayers and octadecanethiol phosphatidyl choline bilayers, J. Electroanal. Chem. 500 (2001) 395–407.
[21] A. Nelson, Effect of lipid charge and solution composition on the permeability of phospholipid–gramicidin monolayers to Tl^{I}, J. Chem. Soc. Faraday Trans. 15 (1993) 2799–2805.
[22] M. Rueda, I. Navarro, G. Ramirez, F. Prieto, C. Prado, A. Nelson, Electrochemical impedance study of Tl^{+} reduction through gramicidin channels in self-assembled gramicidin-modified dioleoylphosphatidylcholine monolayers on mercury electrodes, Langmuir 15 (1999) 3672–3678.
[23] M. Rueda, I. Navarro, C. Prado, C. Silva, Impedance study of Tl^{+} reduction at gramicidin-modified dioleoylphosphatidylcholine-coated mercury electrodes: influence of gramicidin concentration and the nature of the supporting electrolyte, J. Electrochem. Soc. 148 (2001) E139–E147.
[24] M.R. Moncelli, L. Becucci, A. Nelson, R. Guidelli, Electrochemical modeling of electron and proton transfer to ubiquinone-10 in a self-assembled phospholipid monolayer, Biophys. J. 70 (1996) 2716–2726.
[25] G.J. Gordillo, D.J. Schiffrin, The electrochemistry of ubiquinone-10 in a phospholipid model membrane, Faraday Disc. 116 (2000) 89–107.
[26] S.L. Horswell, V. Zamlynny, H-Q. Li, A.R. Merrill, J. Lipkowski, Electrochemical and PM-IRRAS studies of potential controlled transformations of phospholipid layers on Au(111) electrodes, Faraday. Discuss. 121 (2002) 405–422.
[27] I. Zawisza, A. Lachenwitzer, V. Zamlynny, S.L. Horswell, J.D. Goddard, J. Lipkowski, Electrochemical and photon polarization modulation infrared reflection absorption spectroscopy study of the electric field driven transformations of a phospholipid bilayer supported at a gold electrode surface, Biophys. J. 86 (2003) 4055–4075.
[28] X. Bin, I. Zawisza, J.D. Goddard, J. Lipkowski, Electrochemical and PM-IRRAS studies of the effect of the static electric field on the structure of the DMPC bilayer supported at a Au(111) electrode surface, Langmuir 21 (2005) 330–347.
[29] I. Zawisza, X. Bin, J. Lipkowski, Potential-driven structural changes in Langmuir-Blodgett DMPC bilayers determined by in situ spectroelectrochemical PM IRRAS, Langmuir 23 (2007) 5180–5194.
[30] I. Zawisza, M. Nullmeier, S.E. Pust, R. Boukherroub, S. Szunerits, G. Wittstock, Application of thin titanium/titanium oxide layers deposited on gold for infrared reflection absorption spectroscopy: Structural studies of lipid bilayers, Langmuir 24 (2008) 7378–7387.
[31] A. Dicko, H. Bourque, M. Pezolet, Study by infrared spectroscopy of the conformation of dipalmitoylphosphatidylglycerol monolayers at the air-water interface and transferred on solid substrates, Chem. Phys. Lipids 96 (1998) 125–139.
[32] R.V. Duevel, R.M. Corn, M.D. Liu, C.R. Leidner, Orientation and organization in functionalized phospholipid monolayers at gold surfaces as measured by polarization modulation Fourier-transform infrared-spectroscopy, J. Phys. Chem. 96 (1992) 468–473.
[33] J. Liu, J.C. Conboy, 1,2-diacyl-phosphatidylcholine flip-flop measured directly by sum-frequency vibrational spectroscopy, Biophys. J. 89 (2005) 2522–2532.
[34] J. Liu, J.C. Conboy, Direct measurement of the transbilayer movement of phospholipids by sum-frequency vibrational spectroscopy, J. Am. Chem. Soc. 126 (2004) 8376–8377.
[35] J. Liu, J.C. Conboy, Phase transition of a single lipid bilayer measured by sum-frequency vibrational spectroscopy, J. Am. Chem. Soc. 126 (2004) 8894–8895.
[36] Z.V. Feng, T.A. Spurlin, A.A. Gewirth, Direct visualization of asymmetric behavior in supported lipid bilayers at the gel-fluid phase transition, Biophys. J. 88 (2005) 2154–2164.
[37] I. Reviakine, A. Brisson, Formation of supported phospholipid bilayers from unilamellar vesicles investigated by atomic force microscopy, Langmuir 16 (2000) 1806–1815.
[38] B.W. Koenig, S. Kruger, W.J. Orts, C.F. Majkrzak, N.F. Berk, J.V. Silverton, K. Gawrisch, Neutron reflectivity and atomic force microscopy studies of a lipid bilayer in water adsorbed to the surface of a silicon single crystal, Langmuir 12 (1996) 1343–1350.
[39] M. Chen, M. Li, C.L. Brosseau, J. Lipkowski, AFM studies of the effect of temperature and electric field on the structure of a DMPC-cholesterol bilayer supported on an Au(111) electrode surface, Langmuir 25 (2009) 1028–1037.
[40] Z.V. Leonenko, A. Carnini, D.T. Cramb, Supported planar bilayer formation by vesicle fusion: the interaction of phospholipid vesicles with surfaces and the effect of gramicidin on bilayer properties using atomic force microscopy, Biochim. Biophys. Acta 1509 (2000) 131–147.
[41] S. Xu, G. Szymanski, J. Lipkowski, Self-assembly of phospholipid molecules at a Au(111) electrode surface, J. Am. Chem. Soc. 126 (2004) 12276–12277.
[42] S. Sek, T. Laredo, J.R. Dutcher, J. Lipkowski, Molecular resolution imaging of an antibiotic peptide in a lipid matrix, J. Am. Chem. Soc. 131 (2009) 6439–6444.
[43] I. Burgess, M. Li, S.L. Horswell, G. Szymanski, J. Lipkowski, J. Majewski, S. Satija, Electric field-driven transformations of a supported model biological membrane — An electrochemical and neutron reflectivity study, Biophys. J. 86 (2004) 1763–1776.
[44] A.R. Hillman, K.S. Ryder, E. Madrid, A.W. Burley, R.J. Wiltshire, J. Merotra, M. Grau, S.L. Horswell, A. Glidle, R.M. Dalgliesh, A. Hughes, R. Cubitt, A. Wildes, Structure and dynamics of phospholipid bilayer films under electrochemical control, Faraday Discuss. 145 (2010) 357–379.
[45] H.Y. Jing, D.H. Hong, B.D. Kwak, D.J. Choi, K. Shin, C-J. Yu, J.W. Kim, D.Y. Noh, Y.S. Seo, X-ray reflectivity study on the structure and phase stability of mixed phospholipid multilayers, Langmuir 25 (2009) 4198–4202.
[46] A.F. Xie, R. Yamada, A.A. Gewirth, S. Granick, Materials science of the gel to fluid phase transition in a supported phospholipid bilayer, Phys. Rev. Lett. 89 (2002) 246103.
[47] L.K. Tamm, H.M. McConnell, Supported phospholipid-bilayers, Biophys. J. 47 (1985) 105–113.
[48] J.M. Crane, L.K. Tamm, Role of cholesterol in the formation and nature of lipid rafts in planar and spherical model membranes, Biophys. J. 86 (2004) 2965–2979.
[49] A. Barnett, J.C. Weaver, Electroporation: a unified, quantitative theory of reversible electrical breakdown and mechanical rupture in artificial planar bilayer membranes, J. Electroanal. Chem. Bioelectrochem. Bioenerg. 25 (1991) 163–182.
[50] J. Gehl, Electroporation: theory and methods, perspectives for drug delivery, gene therapy and research, Acta Physiol. Scand. 177 (2003) 437–447.
[51] M. Cheever, M. Overduin, in Modular Protein Domains Ed. Cesareni, Wiley 2004.
[52] H.L. Casal, H.H. Mantsch, Infrared studies of fully hydrated saturated phosphatidylserine bilayers. Effect of Li^{+} and Ca^{2+}, Biochemistry 26 (1987) 4408–4416.
[53] S. Choi, W. Ware, S.R. Lauterbach, W.M. Phillips, Infrared spectroscopic studies on the phosphatidylserine bilayer interacting with calcium ion: effect of cholesterol, Biochemistry 30 (1991) 8563–8568.
[54] E. Madrid, S.L. Horswell, Effect of headgroup on the physicochemical properties of phospholipid bilayers in electric fields: size matters, Langmuir 29 (2013) 1695–1708.
[55] H.I. Petrache, S. Tristram-Nagle, K. Gawrisch, D. Harries, V.A. Parsegian, J.F. Nagle, Structure and fluctuations of charged phosphatidylserine bilayers in the absence of salt, Biophys. J. 86 (2004) 1574–1586.
[56] R.A. Demel, F. Paltauf, H.H. Hauser, Monolayer characteristics and thermal behavior of natural and synthetic phosphatidylserines, Biochemistry 26 (1987) 8659–8665.
[57] J. Richer, J. Lipkowski, Measurement of physical adsorption of neutral organic species at solid electrodes, J. Electrochem. Soc. 133 (1986) 121–128.
[58] R. Jackson, V. Zamlynny, Optimization of electrochemical infrared reflection absorption spectroscopy using Fresnel equations, Electrochim. Acta 53 (2008) 6768–6777.
[59] V. Zamlynny, J. Lipkowski, in: R.C. Alkire, D.M. Kolb, J. Lipkowski, P.N. Ross (Eds.), Diffraction and Spectroscopic Methods in Electrochemistry, Wiley-VCH, 2006, Ch.9.
[60] Fresnel1 software written by V. Zamlynny, contact details: Vlad.Zamlynny@AcadiaU.ca
[61] B.J. Barner, M.J. Green, E.I. Saez, R.M. Corn, Polarization Modulation Fourier-Transform Infrared Reflectance measurements of thin-films and monolayers at metal-surfaces utilizing real-time sampling electronics, Anal. Chem. 63 (1991) 55–60.
[62] M.J. Green, B.J. Barner, R.M. Corn, Real-time sampling electronics for double modulation experiments with Fourier-Transform Infrared spectrometers, Rev. Sci. Instrum. 62 (1991) 1426–1430.
[63] T. Buffeteau, B. Desbat, D. Blaudez, J.M. Turlet, Calibration procedure to derive IRRAS spectra from PM-IRRAS spectra, Appl. Spectrosc. 54 (2000) 1646–1650.
[64] V. Zamlynny, I. Zawisza, J. Lipkowski, PM FTIRRAS studies of potential-controlled transformations of a monolayer and a bilayer of 4-pentadecylpyridine, a model surfactant, adsorbed on a Au(111) electrode surface, Langmuir 19 (2003) 132–145.
[65] J. Lipkowski, L. Stolberg, L. in Adsorption of Molecules at Metal Electrodes, J., Lipkowski, P. N. Ross, (Eds.) VCH, New York, 1992, pp. 171-238.
[66] I. Burgess, V. Zamlynny, G. Szymanski, J. Lipkowski, J. Majewski, G. Smith, S. Satija, R. Ivkov, Electrochemical and neutron reflectivity characterization of dodecyl sulfate adsorption and aggregation at the gold–water interface, Langmuir 17 (2001) 3355–3367.
[67] H.L. Casal, H.H. Mantsch, Polymorphic phase behaviour of phospholipid membranes studied by infrared spectroscopy, Biochim. Biophys. Acta 779 (1984) 381–401.
[68] R.N.A.H. Lewis, R.N. McElhaney, Calorimetric and spectroscopic studies of the polymorphic phase behavior of a homologous series of n-saturated 1,2-diacyl phosphatidylethanolamines, Biophys. J. 64 (1993) 1081–1096.
[69] H.L. Casal, H.H. Mantsch, The thermotropic phase behavior of *N*-methylated dipalmitoylphosphatidylethanolamines, Biochim. Biophys. Acta 735 (1983) 387–396.
[70] H.H. Mantsch, S.C. Hsi, K.W. Butler, D.G. Cameron, Studies on the thermotropic behavior of aqueous phosphatidylethanolamines, Biochim. Biophys. Acta 728 (1983) 325–330.
[71] D.G. Cameron, H.L. Casal, H.H. Mantsch, Characterization of the pretransition in 1,2-dipalmitoyl-sn-glycero-3-phosphocholine by Fourier Transform Infrared Spectroscopy, Biochemistry 19 (1980) 3665–3672.
[72] R.G. Snyder, G.L. Liang, H.L. Strauss, R. Mendelsohn, IR spectroscopic study of the structure and phase behavior of long-chain diacylphosphatidylcholines in the gel state, Biophys. J. 71 (1996) 3186–3319.
[73] J. Umemura, D.G. Cameron, H.H. Mantsch, A Fourier-transform infrared spectroscopic study of the molecular interaction of cholesterol with 1,2-dipalmitoyl-sn-glycero-3-phosphocholine, Biochim. Biophys. Acta 602 (1980) 32–44.
[74] H.H. Mantsch, R.M. McElhaney, Phospholipid phase transitions in model and biological membranes as studied by infrared spectroscopy, Chem. Phys. Lipids 57 (1991) 213–226.
[75] E. Okamura, J. Umemura, T. Takenaka, Fourier-transform infrared-attenuated total reflection spectra of dipalmitoylphosphatidylcholine monomolecular films, Biochim. Biophys. Acta 812 (1985) 139–146.

[76] R.N.A.H. Lewis, R.N. McElhaney, Calorimetric and spectroscopic studies of the thermotropic phase behavior of lipid bilayer model membranes composed of a homologous series of linear saturated phosphatidylserines, Biophys. J. 79 (2000) 2043–2055.
[77] W. Hübner, H.H. Mantsch, F. Paltauf, H. Hauser, Conformation of phosphatidylserine in bilayers as studied by Fourier Transform Infrared Spectroscopy, Biochemistry 33 (1994) 320–326.
[78] R.A. Dluhy, D.G. Cameron, H.H. Mantsch, R. Mendelsohn, Fourier Transform Infrared Spectroscopic studies of the effect of calcium ions on phosphatidylserine, Biochemistry 22 (1983) 6318–6325.
[79] R.G. Snyder, S.L. Hsu, S. Krimm, Vibrational-spectra in C-H stretching region and structure of polymethylene chain, Spectrochim. Acta A 34 (1978) 395– 406.
[80] M. Moskovits, Surface selection-rules, J. Chem. Phys. 77 (1982) 4408– 4416.
[81] D.L. Allara, R.G. Nuzzo, Spontaneously Organized Molecular Assemblies. 2. Quantitative Infrared Spectroscopic Determination of Equilibrium Structures of Solution-Adsorbed *n*-Alkanoic Acids on an Oxidized Aluminium Surface, Langmuir 1 (1985) 52–66.
[82] D.L. Allara, J.D. Swalen, An Infrared Reflection Spectroscopy Study of Oriented Cadmium Arachidate Monolayer Films on Evaporated Silver, J. Phys. Chem. 86 (1982) 2700–2704.
[83] J. Umemura, T. Kamata, T. Kawai, T. Takenaka, Quantitative Evaluation of Molecular Orientation in thin Langmuir-Blodgett Films by FT-IR Transmission and Reflection-Absorption Spectroscopy, J. Phys. Chem. 94 (1990) 62–67.
[84] A. Blume, W. Hübner, G. Messner, Fourier Transform Infrared Spectroscopy of $^{13}C=O$-labeled phospholipids hydrogen bonding to carbonyl groups, Biochemistry 27 (1988) 8239–8249.
[85] R.N.A.H. Lewis, R.N. McElhaney, W. Pohle, H.H. Mantsch, Components of the Carbonyl Stretching Band in the Infrared Spectra of Hydrated 1,2-Diacylglycerolipid Bilayers: A Reevaluation, Biophys. J. 67 (1994) 2367–2375.
[86] H.L. Casal, A. Martin, H.H. Mantsch, F. Paltauf, H. Hauser, Infrared studies of fully hydrated unsaturated phosphatidylserine bilayers, Effect of Li^+ and Ca^{2+}, Biochemistry 26 (1987) 7395–7401.
[87] W. Yan, H.L. Strauss, R.G. Snyder, Conformation of the acyl chains in diacylphospholipid gels by IR spectroscopy, J. Phys. Chem. B 104 (2000) 4229–4238.
[88] T. Ishioka, W. Yan, H.L. Strauss, R.G. Snyder, Normal mode analyses of methyl palmitate all-trans and disordered forms in wagging progressive region, Spectrochim. Acta A 59 (2003) 671–680.
[89] C.H. Chen, Interactions of lipid vesicles with solvent in heavy and light water, J. Phys. Chem. 86 (1982) 3559–3562.
[90] U.P. Fringeli, Biophys. J. 34 (1981) 173–187.